Supercritical CO_2/Ionic Liquid Systems: What Can We Extract from Infrared and Raman Spectra?

Jean-Michel Andanson, Fabian Jutz, and Alfons Baiker*

Institute for Chemical and Bioengineering, Department of Chemistry and Applied Biosciences, ETH Zurich, Hönggerberg, HCI, CH-8093 Zürich, Switzerland

Received: May 13, 2009

Infrared (IR) spectroscopy has been successfully applied to study the solubility of supercritical (sc) CO_2 in an ionic liquid (IL), the swelling of the IL under $scCO_2$, the diffusion of CO_2 in the IL, and the molecular interaction between the IL and $scCO_2$ using a single defined experimental setup. The study has been performed using 1-butyl-3-methylimidazolium hexafluorophosphate [bmim][PF_6] and $scCO_2$ with a pressure of up to 150 bar at 313 K. The solubility of $scCO_2$ in the IL was calculated via the intensity of the CO_2 antisymmetric stretching mode, which was measured using the attenuated total reflection (ATR) method. This approach allowed to determine also the swelling of the IL under $scCO_2$ using several IL bands. The knowledge gained about the solubility and swelling allowed the calculation of the molar fraction of CO_2 in the IL and the attainment of similar data as previously determined by other methods. The kinetic measurement of the infrared spectra also offered the opportunity to observe the evolution of the concentration of CO_2 in the IL and allowed an estimation of the diffusion coefficient of CO_2 in IL under high pressure. Finally, information about the molecular interactions between the IL and $scCO_2$ could also be gained in situ using both infrared and Raman spectroscopy.

1. Introduction

Ionic liquids (ILs) are defined as salts with a melting point below the boiling point of water.[1] Within this group, salts that are liquid already at room temperature are called room-temperature ionic liquids (RTILs). Due to their peculiar properties, such as their negligible vapor pressure, ILs and RTILs have gained considerable attention in research and application, e.g. for supported ionic liquid phase (SILP) catalyst systems or multiphase reactions. Especially interesting seems the combination of ILs with carbon dioxide, because ILs are not soluble in CO_2, whereas CO_2 is soluble in ILs. The critical temperature and pressure of CO_2 are 304 K and 74 bar, respectively. Supercritical CO_2 ($scCO_2$) can be defined as a fluid with a temperature above the critical temperature. As $scCO_2$ is inexpensive, nontoxic, nonpolluting, and easily removable, it is widely used as cleaning or separation agent, as solvent, or increasingly also as reactant. By changing the pressure and the temperature of the system, it is possible to tune the solvent power of $scCO_2$ and to adjust it to the requirements of an application. Using both IL and $scCO_2$ in the same system offers broad possibilities for new chemical processes. Some of the applications of binary IL−$scCO_2$ systems, e.g. for extraction or chemical reactions, have just been reviewed by Roth.[2] The melting point depression of several organic salts is also well explained in this review. As $scCO_2$ is decreasing the melting point, some organic salts can become liquid at much lower temperature (some melting point depressions can exceed 100 K[3,4]), and in this case, some salts can also be used as ILs in an IL−$scCO_2$ system. Spectroscopy can be used to study in situ the properties of these new systems, and some recent studies of combined spectroscopic techniques under high pressure have been reviewed by Tinnemans et al.[5] However, a complete understanding of IL−$scCO_2$ systems is still far from being reached and would greatly help in optimizing chemical process development utilizing IL−$scCO_2$ systems. A few years ago, Kazarian and co-workers presented several studies showing the opportunity of in situ attenuated total reflection Fourier transform infrared (ATR-FTIR) in this field.[6–8] In the wide range of spectroscopic techniques, ATR-FTIR appears to be one of the most promising ones by its ability to measure thermodynamic and kinetic properties as well as molecular interactions.[9]

Recently, our group studied the interaction of 1-*n*-butyl-3-methylimidazolium tetrafluoroborate [bmim][BF_4], 1-*n*-butyl-3-methylimidazolium hexafluorophosphate [bmim][PF_6], 1-*n*-butyl-3-methylimidazolium bis(trifluoromethylsulfonyl)imide [bmim][Tf_2N], and 1-*n*-butylpyridinium tetrafluoroborate [bpy][BF_4] with $scCO_2$ at 323 K and 120 bar using ATR-FTIR in situ spectroscopy,[10] focusing mainly on the chemical interaction between the IL and CO_2 and a qualitative analysis of the system. The peak areas of the antisymmetric stretching band of CO_2 were used to compare qualitatively the solubility of CO_2 in different ILs at 323 K and 120 bar.

In the present study, we focused on the quantitative analysis of the binary system [bmim][PF_6] and $scCO_2$. Using the ATR spectra, molecular interactions between IL and $scCO_2$ were investigated. Raman spectra of [bmim][PF_6]/CO_2 were also recorded to obtain complementary information of any molecular interactions in this system. The system [bmim][PF_6] was selected for this study because it is one of the most widely used and most intensively studied ILs, as reflected by the extensive thermodynamic data of ILs (pure, binary, and ternary mixtures) published by NIST.[11] Our data obtained from ATR-FTIR experiments at 313 K up to 150 bar is compared to the literature to validate our approach. The advanced analysis of these spectra allowed us to calculate the solubility of $scCO_2$ in the IL and the compressibility and the swelling of the IL under $scCO_2$. The kinetic measurement of the infrared spectra also gave the

* To whom correspondence should be addressed. E-mail: baiker@chem.ethz.ch. Phone: +41 44 632 31 53. Fax: +41 44 632 11 63.

10.1021/jp904440x CCC: $40.75
Published on Web 07/02/2009

opportunity to observe the evolution of the concentration of CO_2 in the IL during the diffusion process and to estimate the diffusion coefficient of CO_2 in IL under high pressure.

2. Experimental Details

For the spectroscopic experiments, a high pressure cell with variable volume and several optical probing paths was used. The cell is equipped with two sapphire windows to observe directly the phase behavior and to introduce the Raman laser. Furthermore, it is equipped with two ZnSe windows for transmission infrared measurements mainly in the gas phase and an ATR-FTIR crystal on the bottom to study the liquid phase. The details of the cell used in this work are described elsewhere.[12] A rectangular PTFE ring was used as sealing between the multiple reflections ZnSe (or Ge) ATR crystal and the cell to avoid any leaking. FTIR spectra were measured with an IFS-66 spectrometer (Bruker Optics) with a resolution of 2 cm^{-1}. A high quality signal-to-noise ratio (s/n) was obtained in the range of 4000−600 cm^{-1} using 128 scans with a liquid nitrogen cooled mercury cadmium telluride (MCT) detector. Raman spectra (range of 200−2000 cm^{-1}) were obtained using a QE65000 spectrometer by Ocean optics with 785 nm laser excitation and an integration time of 100 s. The [bmim][PF_6] was purchased from ABCR (99% purity, product no. AB172327) while CO_2 was delivered from Pangas (99.995% purity).

In the case where the used internal reflection element (IRE) was a ZnSe crystal, the evolution of the spectra of the IL−$scCO_2$ system was measured on the 313 K (±1 K) isotherm up to 150 bar (±1 bar), while the maximum pressure was 80 bar in the case where a Ge crystal was employed. For safety reasons, it was decided to not perform an experiment with higher pressure than this, as the rupture modulus of Ge is less than 1000 bar. Before any experiment, the IL was dried under vacuum at 1.0 Pa at 333 K for 48 h, as traces of water in [bmim][PF_6] were found to affect the IL−$scCO_2$ equilibrium.[13,14] A precise amount of 0.2−0.3 g of IL was placed on the top surface of the ATR crystal, forming a layer of typically 2−3 mm of IL inside the cavity of the high pressure cell. The quantity of IL was kept minimal to allow a relatively fast experiment, as the CO_2 should diffuse through the IL. On the other hand, much care was taken to ensure a full coverage of the IL on the crystal at all times of the experiment, to be able to calculate reliable quantitative data from the evolution of the spectra. The experiment was started by adding N_2 to [bmim][PF_6] up to a pressure of 80 bar to ensure an optimal contact between the IL layer and the ATR crystal. Afterward, N_2 was released and the IL was left for 1 h under 1 bar of N_2. Finally, CO_2 was introduced into the cell and flushed to remove the N_2, and the pressure was increased up to the first experimentally desired pressure (10 bar). A spectrum was recorded every 5 min until the equilibrium was reached. For the lowest pressure, it took over 3 h to achieve the equilibrium. Before any further increase in pressure on the isotherm, the system was left for at least 1 h. The experiment was performed both with and without a magnetic stirrer in the liquid phase, and experiments done without a stirrer could be used to calculate kinetic parameters of the system under high pressure. It should be mentioned that the diffusion of CO_2 in [bmim][PF_6] is improved a lot with the use of a stirrer; however, it is much easier to observe the equilibration of the system when it is not stirred. In our case, the use of the stirrer resulted in around 90−95% of the CO_2 being dissolved in the IL in less than 20 min, while it took over 2 h to finally achieve equilibrium.

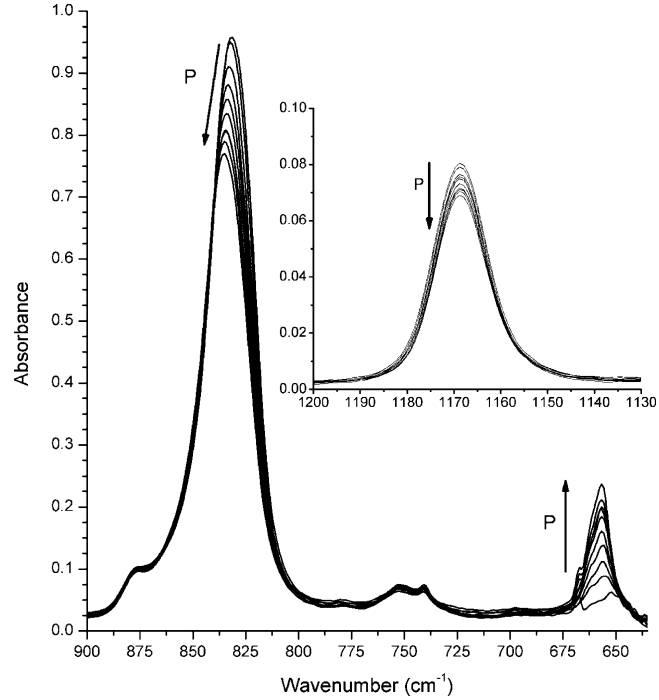

Figure 1. Infrared spectra of [bmim][PF_6] under pressure of CO_2 (0, 10, 20, ..., 80 bar) at 313 K using a Ge crystal.

3. Results and Discussion

3.1. Molecular Interaction between IL and CO_2. ATR-FTIR spectra of [bmim][PF_6] under $scCO_2$ have already been published previously for different pressures and temperatures.[8,10] In our study, the evolution of a part of the IR spectra with the pressure of CO_2 at 313 K is presented in Figure 1. In IR, the main bands of CO_2 in the mid-IR region are the asymmetric stretching mode at 2338 cm^{-1} and the bending mode at 660 cm^{-1}. The CO_2 bands are increasing with rising pressure, while the IL bands are slightly decreasing. The broad and complex band situated around 810−850 cm^{-1}, which can be attributed to a vibration of the [PF_6] group, is the only band which is showing a noticeable shift with increasing concentration of CO_2 in the IL. The structure of the [bmim][PF_6]−CO_2 system at 298 K has been explored by means of molecular dynamics simulations and reported by Bhargava and Balasubramanian.[15] The most prominent effect of the insertion of CO_2 molecules into IL is the large decrease of the anion−anion coordination number at 8 Å distance (from 5.4 in the pure liquid to 3.2 molecules in the mixture). The variation of the average organization between cation−cation and cation−anion is much smaller. Another theoretical study, using ab initio calculations, has demonstrated the effect of the presence of a cation close to the PF_6^- anion on the position and intensity of the PF_6^- symmetric stretching mode.[16] With a DFT (density functional theory) method at the B3LYP/6-311+G(2df) level, the frequency of the symmetric stretching of the PF_6^- ion is located at 834.4 cm^{-1}, while the same vibration is shifted to 891.9 cm^{-1} for the $Li^+PF_6^-$. For that reason, the shift of the PF_6^- band observed with increasing pressure could be the result of the increase of the distance between the anions and cations or between anions, but not necessarily of an interaction between CO_2 and PF_6^-. The CO_2 asymmetric stretching and the CO_2 bending modes are shifted from 2333 to 2340 cm^{-1} and from 660 to 656 cm^{-1} between pure CO_2 and CO_2 dissolved in [bmim][PF_6], respectively, and the position of the CO_2 asymmetric stretching mode is slightly sensitive to the pressure of the system, while it was not possible

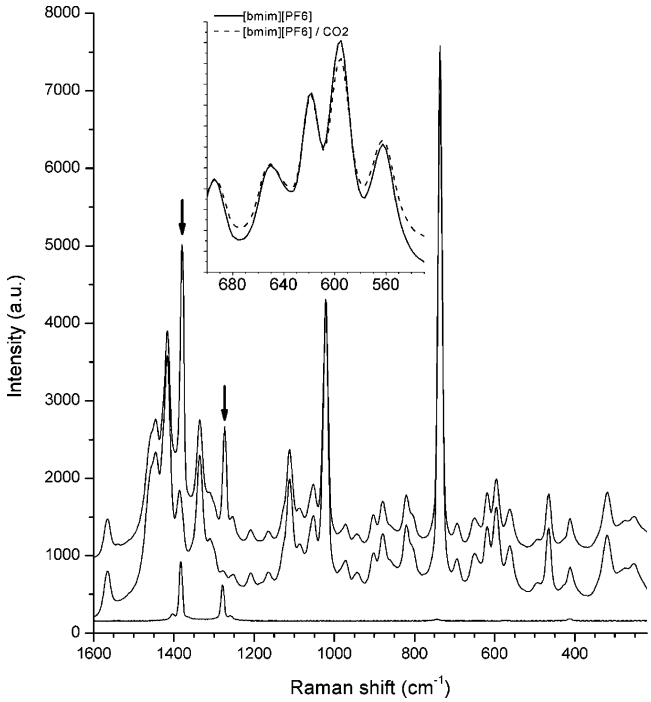

Figure 2. Raman spectra of the [bmim][PF_6]−CO_2 system at 313 K. From top to bottom: (1) [bmim][PF_6]−CO_2 at 140 bar. (2) [bmim][PF_6] without CO_2. (3) Pure CO_2. Arrows indicate the main bands of CO_2.

to observe any shift of the bending mode. The shift of the stretching mode to lower frequency is probably due to the decrease of the density of the liquid phase with increasing pressure.

The Raman spectra of [bmim][PF_6]−$scCO_2$ (at 140 bar), pure [bmim][PF_6], and pure CO_2 under high pressure at 313 K are presented in Figure 2. The main effect of CO_2 on the spectra of [bmim][PF_6] is the appearance of the CO_2 vibrations in the spectra. Except that, the main difference is a change of the ratio between the two bands situated around 600 and 620 cm^{-1}. Hamaguchi and Ozawa measured the Raman spectra of gauche and trans configurations of $bmim^+$ in various ILs.[17] The band at 626 cm^{-1} was assigned to a trans configuration, while the band at 596 cm^{-1} was attributed to the same vibration in gauche configuration of the butyl group of the cation. Later, Holomb et al. studied the evolution of the ratio between gauche and trans conformers with the temperature in [bmim][BF_4].[18] We found a similar change in the ratio of these two conformers with increasing pressure of CO_2, as shown in Figure 2. The relative amount of the trans configuration increased proportionally with the pressure of CO_2. This result is not surprising, as the IL is swelling and the density is decreasing when the pressure of CO_2 increases. The presence of CO_2 facilitates the sterically more demanding trans conformation of the butyl group.

Nevertheless, the shift of the PF_6^- stretching mode in the infrared spectra and a small change of the trans/gauche ratio, detected with Raman spectroscopy, are the only changes of the spectra while CO_2 is dissolved in [bmim][PF_6]. Therefore, we can conclude that the structure of the IL is mainly conserved, and only minor reconfiguration is involved during the dissolution of CO_2 in [bmim][PF_6] under high pressure.

3.2. IL Swelling under $scCO_2$. Flichy et al. have demonstrated the opportunity to measure simultaneously the solubility of CO_2 in a polymer and the swelling of the polymer.[19] The swelling of the polymer was calculated with the evolution of the intensity of the band of the polymer,

$$S = \frac{A^\circ}{A}\frac{d_{e,u}}{d^\circ_{e,u}} - 1 \quad (1)$$

where S is the swelling, A, $d_{e,u}$, A°, and $d^\circ_{e,u}$ are the absorbance and the effective thickness with and without pressure, respectively.

For our experimental setup, following the approach used in ref 20, the effective thickness of pure [bmim][PF_6] ($d^\circ_{e,u}$) is 1.180 μm when a ZnSe ATR crystal is used, and 0.2824 μm with a Ge crystal for the CH stretching band. The effective thickness is much bigger at lower wavelengths, 1.049 μm for the PF_6^- vibration at 830 cm^{-1} with a Ge crystal (the absorption of this vibration was too strong when using ZnSe as IRE to be able to use it for quantitative analysis). In order to obtain these values, the refractive index of ZnSe (2.42), Ge (4.00), and IL (1.4046 at 313 K[21]), the angle of incidence (60°), and the number of reflections ($n = 3$) are required. Due to the swelling, a probable decrease of the refractive index of a few percents is expected. Flichy et al. have demonstrated the opportunity to calculate the variation of the refractive index of the sample with the evolution of the absorbance under the same conditions, using two different IREs and an incident angle of 45°. They showed a negligible effect of the variation of the refractive index on the value of the swelling. In our case, with an incident angle of 60°, which is even further from the critical angle, the variation of the refractive index of a few percent will induce an even more negligible decrease of the effective thickness. In fact, in our case, it was not even possible to calculate accurately the variation of the refractive index with the pressure of CO_2. Consequently, the swelling was calculated directly with the variation of the absorbance.

The swelling of [bmim][PF_6] under $scCO_2$ has already been studied with other techniques by several groups[13,14,22] up to 150 bar. Our results obtained by infrared spectroscopy, using two different crystal materials and two different bands, are compared in Figure 3 to the results of Aki et al., who used a stoichiometric phase equilibrium apparatus.[13] All the results obtained from the two different crystals and the selected vibrational bands are in a good agreement. Despite the shift of the PF_6^- stretching band, it seems that this band can be used to quantify the swelling of the IL. The comparison between our spectroscopic data and the literature reveals a good agreement for the lower pressures (below 40 bar). For these pressures, the swelling increases linearly with the pressure while CO_2 molecules are absorbed easily in the IL. On the other hand, when the pressure is higher than 80 bar, the effect of the pressure on the swelling of the IL is much smaller and our data seems to agree only partially with the values measured by Aki et al.

3.3. CO_2 Solubility in IL. The solubility of $scCO_2$ in [bmim][PF_6] has been studied by several groups using a gravimetric microbalance[23–25] or phase equilibration.[13] Infrared spectroscopy could also be used to quantify this solubility by using the absorbance of the asymmetric stretching mode at 2335 cm^{-1}. Flichy et al. calculated the solubility of CO_2 using ATR-FTIR spectra on noncross-linked poly(dimethylsiloxane),[19] while Pasquali et al. also applied this to solid and liquid poly(ethylene glycol)−$scCO_2$ systems.[20] To calculate the amount of CO_2 in the present work, we used the absorbance of the 2338 cm^{-1} band, which was quantified by measuring the height of the relevant peak and using the molar absorptivity of high-pressure CO_2, specifically the value of 1.0×10^6 cm^2 mol^{-1}, determined by Maiella et al.[26] The asymmetric stretching band of CO_2 dissolved in [bmim][PF_6] at different pressures, measured with both ZnSe and Ge crystals, is shown in Figure 4. The effective thicknesses in our system are 1.565 and 0.374 μm for this band

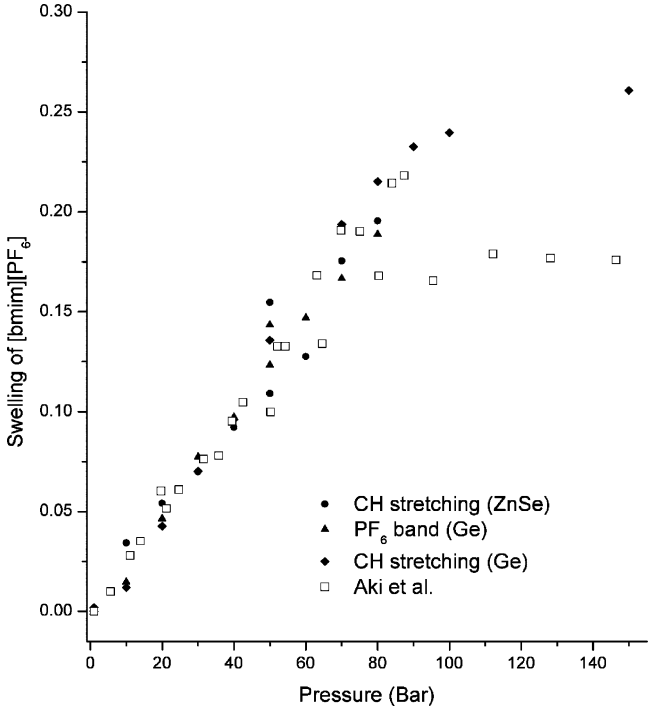

Figure 3. Evolution of the swelling of [bmim][PF_6] as function of the pressure of CO_2 at 313 K, calculated with the intensity of the CH and [PF_6^-] stretching bands, using Ge and ZnSe crystals as internal reflection elements. The intensity of the [PF_6^-] stretching bands using ZnSe is too big to exploit any quantitative information from this band.

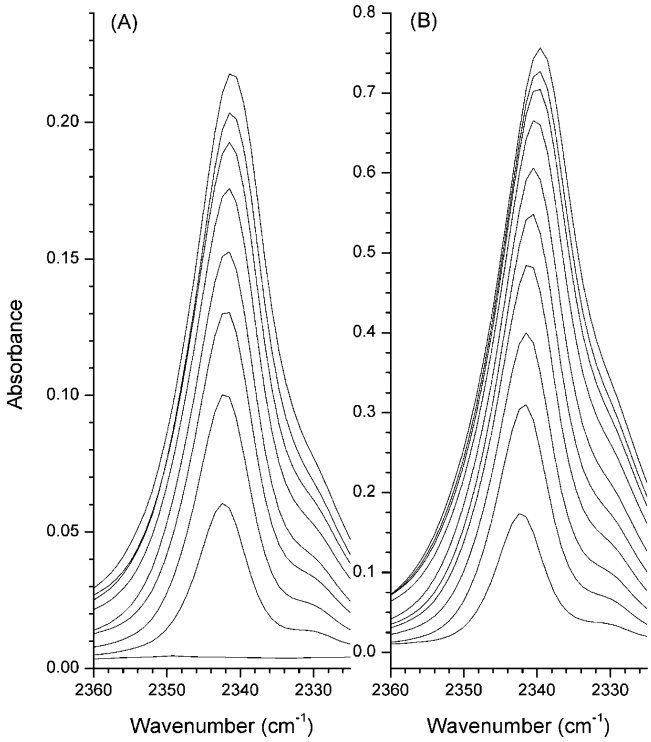

Figure 4. Evolution of the asymmetric stretching band of CO_2 in the [bmim][PF_6]−CO_2 system at 313 K. (A) Increase of the CO_2 pressure from 0, 10, 20, ..., 80 bar using a Ge crystal as the internal reflection element. (B) Increase of the CO_2 pressure at 10, 20, 30, 40, 50, 70, 80, 90, 100, and 150 bar, using a ZnSe crystal as the internal reflection element.

for ZnSe and Ge crystal, respectively. The difference (a factor of 4) in effective thickness explains the difference of intensity observed in Figure 4 with the two different IRE. Using the

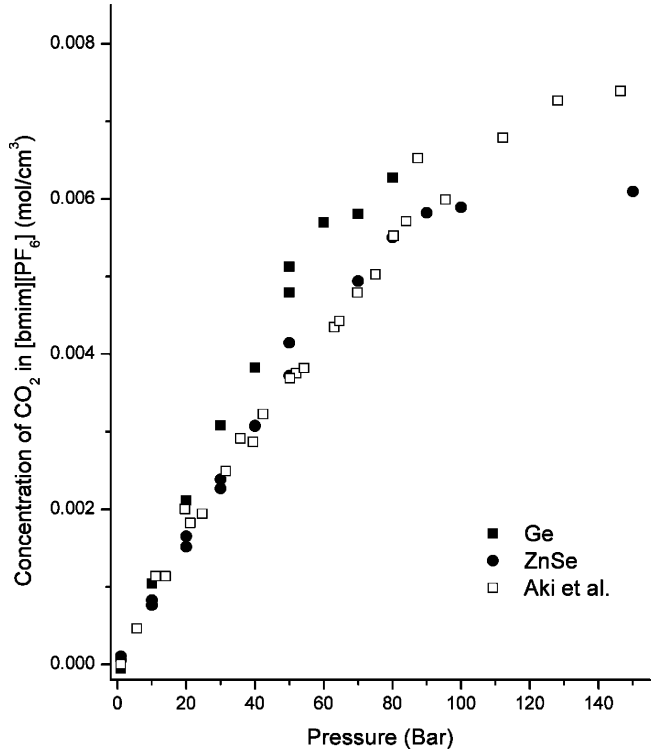

Figure 5. Evolution of the concentration of CO_2 in [bmim][PF_6] at 313 K as function of the pressure of CO_2, calculated with the intensity of the asymmetric stretching band of CO_2, using Ge and ZnSe crystals as the internal reflection element.

effective thickness and the molar absorptivity, it was possible to calculate the solubility of CO_2 in [bmim][PF_6]. The comparison of our infrared spectroscopic measurements with the data obtained by Aki et al. for the solubility is shown in Figure 5. A good agreement was found between the measurements done with both crystals as well as with the data from the literature, except for the higher pressure, where the spectra show only a small increase of the CO_2 concentration, while Aki et al. observed an increase of 20% of the solubility between 90 and 150 bar, and they assumed that their method was less accurate when the variation of solubility with the pressure was smaller. We do not see any explanation why we could have underestimated the concentration of CO_2 at high pressure. The value at 150 bar was taken after 4 h of equilibration, and the spectra at 100 and 150 bar are still almost identical.

The molar fraction of CO_2 in IL could be calculated using the data of swelling and concentration of CO_2 in IL. The results obtained are depicted and compared with the literature[13,27] in Figure 6. In this case even at high pressure, all the data illustrate the same evolution with the pressure. For pressures over 80 bar, a limit of two CO_2 molecules per [bmim][PF_6] is observed. As described in the literature, the anionic species determine this ratio,[13] as CO_2 is mainly interacting with the anion of the IL.[6] In the case of [bmim][PF_6]−CO_2 under high pressure, a simple geometric description of the system would be 1 $bmim^+$ and 2 CO_2 molecules surrounding a PF_6^- molecule.

3.4. Diffusion of CO_2 into IL. The diffusion of CO_2 into [bmim][PF_6] was measured by Shiflett et al. up to 20 bar, using time dependent absorption data obtained with a gravimetric microbalance.[25] However, so far, the evolution of an experimental diffusion coefficient of CO_2 in IL up to higher pressure has not been published. Nevertheless, a molecular dynamics study on [bmim][PF_6] with CO_2 at 300 K for various concentrations of CO_2 showed an increase of the diffusion coefficient of

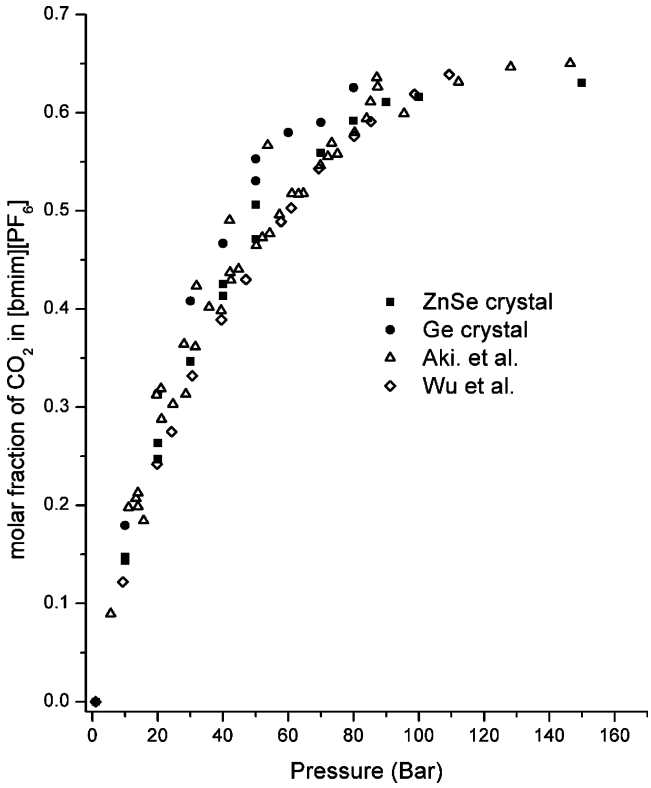

Figure 6. Solubility of CO_2 in [bmim][PF_6] at 313 K.

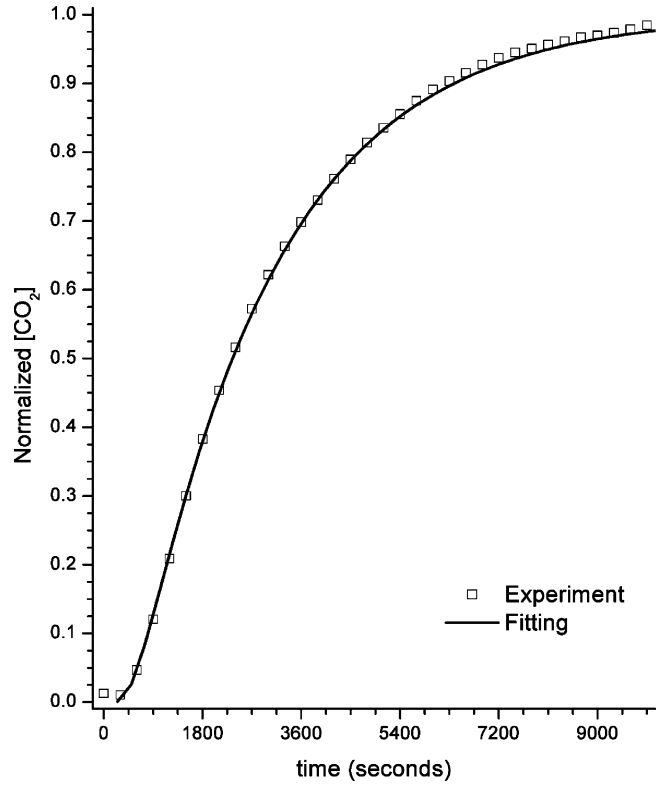

Figure 7. Diffusion of CO_2 in [bmim][PF_6] at 313 K and 20 bar.

CO_2 in the IL from 2.0×10^{-12} to 14.5×10^{-12} m^2 s^{-1} at 0.6 and 150 bar, respectively.[28]

ATR-FTIR spectroscopy was used in several publications to measure the diffusion coefficient of small molecules in polymer films.[29–33] For 1-dimensional molecular diffusion with a constant diffusion coefficient, the continuity equation for the diffusing species reduces to

$$\frac{\partial C}{\partial t} = D\frac{\partial^2 C}{\partial z^2} \tag{2}$$

where C is the concentration of the penetrant and D is the diffusion coefficient. In the case of ATR-IR spectroscopy, Fieldson and Barbari detail the approach of the diffusion in polymer.[33] They considered M_t the mass sorbed at time t, while M_∞ is the mass sorbed at equilibrium for a thickness in 2D

$$\frac{M_t}{M_\infty} = 1 - \sum_{n=0}^{\infty}\left(\frac{8}{(2n+1)^2\pi^2}\right)\exp\left(\frac{-D(2n+1)^2\pi^2 t}{4L^2}\right) \tag{3}$$

and with an approximation for a short time (where $M_t/M_\infty \ll 0.5$):

$$\frac{M_t}{M_\infty} = \frac{2}{L}\left(\frac{D}{\pi}\right)^{1/2} t^{1/2} \tag{4}$$

And accordingly, for a long time (where $M_t/M_\infty \gg 0.5$)

$$\ln\left(1 - \frac{A_t}{A_\infty}\right) = \ln\left(\frac{4}{\pi}\right) - \frac{D\pi^2}{4L^2}t \tag{5}$$

This last equation could be used to fit the CO_2 diffusion in IL kinetics data after a long time (close to the equilibrium). In these equations, L corresponds to half of the thickness of the IL, which is easy to calculate knowing exactly the quantity of IL and the geometry of the cell. However, this model is not taking into account the variation of the refractive index of the material during the diffusion of CO_2, and it can only be used when the penetration depth is much smaller than the thickness of the material (IL in our case). Furthermore, this approach is only valid when the diffusion coefficient is constant with time. Also, if the IL is swelling significantly during the time CO_2 is diffusing inside, these three equations cannot be applied to determine exact diffusion coefficients for all times of the experiment. The value obtained for the diffusion coefficient of the IL is only an estimated value, as the thickness of the liquid is not perfectly constant on the entire surface of the ATR crystal (probable change of meniscus with the change of pressure).

The delay between the increase of the CO_2 pressure in the system and the first appearance of the CO_2 bands in the infrared spectra corresponds to the time needed by the CO_2 to diffuse through the few millimeters of IL. A typical delay of 20 min (as shown in Figure 6) with a 2 mm thickness of IL leads to the calculation of a diffusivity of the CO_2 molecules of 4×10^{-9} m^2 s^{-1}, which corresponds to the diffusion of the "first" molecules arriving on the bottom surface of the IL. In Figure 7, an example of the evolution of the concentration of CO_2 with the time is depicted, while the pressure was increased from ambient pressure to 20 bar at $t = 0$ min. The fitting shown in this example corresponds to the model using the first six terms of eq 3, where both short and long time are taken into account. The estimation of the diffusion coefficient of CO_2 in [bmim][PF_6], at 20 bar and 313 K, obtained from that fitting, is 1×10^{-10} m^2 s^{-1}. This value is equivalent to the data obtained by Shiflett and Yokozeki who used the corresponding equation for the diffusion profiles of CO_2 in IL on gravimetric microbal-

ance data.[25] Our observation on the measurement at higher pressure led us to the assumption that the diffusion coefficient was increasing with pressure. However, at high pressure the model becomes more complex; in this regime, the swelling of the IL layer has to be taken into account and the diffusion coefficient may change drastically with increasing concentration of CO_2. Hence, it is very difficult to extract a diffusion coefficient from our data at higher pressures. In that case, the use of a simpler (or different) model than that described with eq 4 or 5 could help. Nevertheless, this preliminary result is promising, and it should be generally possible to measure the diffusion coefficient of a gas under high pressure in ILs.

3.5. Solubility of IL in the scCO$_2$ Phase. Transmission FTIR spectra (with a few millimeters of path length) of the gas phase of the IL−CO_2 system were measured at several pressures (up to 150 bar) and temperatures (313 and 323 K) under supercritical conditions. No IL, water, or any other impurities were observed in the infrared spectra with an estimated sensitivity of better than 1‰. The analyses of the gas phase could be very useful in the future in the case of ternary systems, such as [bmim][PF_6]−CO_2−methanol studied by Liu et al.[34] This approach was introduced previously by Sakellarios and Kazarian to quantify in situ the solute partitioning between an ionic liquid and high-pressure CO_2.[8]

4. Conclusions

Infrared and Raman spectra of the [bmim][PF_6]−CO_2 system at 313 K and with pressures up to 150 bar were measured. The qualitative analysis of the spectra revealed an increase of the trans conformation of the butyl group in $bmim^+$ with increase of the CO_2 pressure. The infrared spectra demonstrated a shift to higher frequency of the PF_6^- stretching mode. However, the structure of [bmim][PF_6] did not change strongly with the introduction of CO_2 under high pressure. The quantitative analysis of the ATR-FTIR spectra with two different IRE shows a good agreement between our data and the literature at lower pressure (below 80 bar), while some disagreement was found for higher pressure. Nevertheless, in the [bmim][PF_6]−CO_2 system, a molar ratio of 2/3 of CO_2 was found for pressures over 80 bar, and this result is similar to that found in the literature. Finally, for the diffusion coefficient of the CO_2 at 20 bar, a value of 1×10^{-10} m^2 s^{-1} was estimated using the evolution of the concentration of CO_2 on the bottom of the IL layer after a fast increase of pressure. Further work will be required to be able to extract a diffusion coefficient at higher pressure, but these first results prove ATR infrared spectroscopy to be a useful technique to measure the diffusion coefficient of gas molecules into ILs. Apart from analyzing the liquid phase, also the transmission spectra of the gas phase can be recorded and used to quantify substances which are soluble in the scCO$_2$ phase.

Acknowledgment. The financial support from the Bundesamt für Energie (BFE) is greatly appreciated.

References and Notes

(1) Wilkes, J. S. *Green Chem.* **2002**, *4*, 73.
(2) Roth, M. *J. Chromatogr. A* **2009**, *1216*, 1861.
(3) Scurto, A. M.; Leitner, W. *Chem. Commun.* **2006**, 3681.
(4) Scurto, A. M.; Newton, E.; Weikel, R. R.; Draucker, L.; Hallett, J.; Liotta, C. L.; Leitner, W.; Eckert, C. A. *Ind. Eng. Chem. Res.* **2008**, *47*, 493.
(5) Tinnemans, S. J.; Mesu, J. G.; Kervinen, K.; Visser, T.; Nijhuis, T. A.; Beale, A. M.; Keller, D. E.; van der Eerden, A. M. J.; Weckhuysen, B. M. *Catal. Today* **2006**, *113*, 3.
(6) Kazarian, S. G.; Briscoe, B. J.; Welton, T. *Chem. Commun.* **2000**, 2047.
(7) Kazarian, S. G.; Sakellarios, N.; Gordon, C. M. *Chem. Commun.* **2002**, 1314.
(8) Sakellarios, N. I.; Kazarian, S. G. *J. Chem. Thermodyn.* **2005**, *37*, 621.
(9) Stuart, B. *Infrared spectroscopy fundamentals and applications*; J. Wiley: Chichester, West Sussex, England; Hoboken, NJ, 2004.
(10) Seki, T.; Grunwaldt, J.-D.; Baiker, A. *J. Phys. Chem. B* **2009**, *113*, 114.
(11) ILThermo. http://ilthermo.boulder.nist.gov/ILThermo/ (accessed May 2, 2009).
(12) Schneider, M. S.; Grunwaldt, J.-D.; Bürgi, T.; Baiker, A. *Rev. Sci. Instrum.* **2003**, *74*, 4121.
(13) Aki, S. N. V. K.; Mellein, B. R.; Saurer, E. M.; Brennecke, J. F. *J. Phys. Chem. B* **2004**, *108*, 20355.
(14) Blanchard, L. A.; Gu, Z.; Brennecke, J. F. *J. Phys. Chem. B* **2001**, *105*, 2437.
(15) Bhargava, B. L.; Balasubramanian, S. *J. Phys. Chem. B* **2007**, *111*, 4477.
(16) Xuan, X.; Wang, J.; Wang, H. *Electrochim. Acta* **2005**, *50*, 4196.
(17) Hamaguchi, R. O.; Ozawa, H. Structure of Ionic Liquids and Ionic Liquid Compounds: Are Ionic Liquids Genuine Liquids in the Conventional Sense? In *Advances in Chemistry and Physics*; Stuart, A. R., Ed.; Wiley-Interscience: New York, 2005; p 85.
(18) Holomb, R.; Albinsson, A. M., I.; Lassègues, J. C.; Johansson, P.; Jacobsson, P. *J. Raman Spectrosc.* **2008**, *39*, 793.
(19) Flichy, N. M. B.; Kazarian, S. G.; Lawrence, C. J.; Briscoe, B. J. *J. Phys. Chem. B* **2002**, *106*, 754.
(20) Pasquali, I.; Andanson, J.-M.; Kazarian, S. G.; Bettini, R. *J. Supercrit. Fluids* **2008**, *45*, 384.
(21) Kumar, A. *J. Solution Chem.* **2008**, *37*, 203.
(22) Tomida, D.; Kumagai, A.; Qiao, K.; Yokoyama, C. *J. Chem. Eng. Data* **2007**, *52*, 1638.
(23) Anthony, J. L.; Maginn, E. J.; Brennecke, J. F. *J. Phys. Chem. B* **2002**, *106*, 7315.
(24) Cadena, C.; Anthony, J. L.; Shah, J. K.; Morrow, T. I.; Brennecke, J. F.; Maginn, E. J. *J. Am. Chem. Soc.* **2004**, *126*, 5300.
(25) Shiflett, M. B.; Yokozeki, A. *Ind. Eng. Chem. Res.* **2005**, *44*, 4453.
(26) Maiella, P. G.; Schoppelrei, J. W.; Brill, T. B. *Appl. Spectrosc.* **1999**, *53*, 351.
(27) Wu, W.; Li, W.; Han, B.; Jiang, T.; Shen, D.; Zhang, Z.; Sun, D.; Wang, B. *J. Chem. Eng. Data* **2004**, *49*, 1597.
(28) Bhargava, B. L.; Krishna, A. C.; Balasubramanian, S. *AIChE J.* **2008**, *54*, 2971.
(29) Wurster, D. E.; Buraphacheep, V.; Patel, J. M. *Pharm. Res.* **1993**, *10*, 616.
(30) Farinas, K. C.; Doh, L.; Venkatraman, S.; Potts, R. O. *Macromolecules* **1994**, *27*, 5220.
(31) Balik, C. M.; Simendinger, W. H. *Polymer* **1998**, *39*, 4723.
(32) Akon Higuchi, T. N.; Morisato, A.; Ando, M.; Nagai, K.; Nakagawa, T. *J. Polym. Sci. Part B: Polym. Phys.* **1996**, *34*, 2153.
(33) Fieldson, G. T.; Barbari, T. A. *Polymer* **1993**, *34*, 1146.
(34) Zhimin Liu, W. W.; Han, B.; Dong, Z.; Zhao, G.; Wang, J.; Jiang, T.; Yang, G. *Chem.—Eur. J.* **2003**, *9*, 3897.

JP904440X